CH2M-32542-FP
Revision 0

Inhibition of Stress Corrosion Cracking of Carbon Steel Storage Tanks at Hanford

Prepared for the U.S. Department of Energy
Assistant Secretary for Environmental Management

Contractor for the U.S. Department of Energy
Office of River Protection under Contract DE-AC27-99RL14047

CH2MHILL
Hanford Group, Inc.

P.O. Box 1500
Richland, Washington

CH2M-32542-FP
Revision 0

Inhibition of Stress Corrosion Cracking of Carbon Steel Storage Tanks at Hanford

C. S. Brossia
J. A. Beavers
M. P. H. Brongers
C. Scott CC Technologies

G. L. Edgemon
ARES Corporation

G. S. Frankel
Ohio State University

B. Wiersma
Savannah River National Laboratory

H. Berman
Perot Systems Corporation

L. Stock
6695 SW 86th Avenue, Portland, OR 97723

K. D. Boomer
CH2M HILL Hanford Group, Inc.

Date Published
January 2007

To Be Presented at
National Association of Corrosion Engineers 2007 Conference & Exhibition

National Association of Corrosion Engineers
Nashville, TN

March 11-15, 2007

Prepared for the U.S. Department of Energy
Assistant Secretary for Environmental Management

Contractor for the U.S. Department of Energy
Office of River Protection under Contract DE-AC27-99RL14047

CH2MHILL
Hanford Group, Inc.

P.O. Box 1500
Richland, Washington

Approved for Public Release;
Further Dissemination Unlimited

J. D. Aardal 01/31/2007
Release Approval Date

INHIBITION OF STRESS CORROSION CRACKING OF CARBON STEEL STORAGE TANKS AT HANFORD

C.S. Brossia, C. Scott, J.A. Beavers, M.P.H. Brongers
CC Technologies
5777 Frantz Road
Dublin, OH 43017

G.L. Edgemon
ARES Corporation
1100 Jadwin Ave, STE 400
Richland, WA 99352

H. Berman
Perot Systems Corporation
2300 West Plano Parkway
Plano, TX 75075

G.S. Frankel
Ohio State University
477 Watts Hall
2041 College Rd
Columbus, OH 43210

Leon Stock
6695 SW 86th Avenue
Portland, OR 97723

Bruce Wiersma
Savannah River National Laboratory
Aiken, SC 29808

Kayle Boomer
CH2M HILL Hanford Group, Inc.
Richland, WA 99352

ABSTRACT

The stress corrosion cracking (SCC) behavior of A537 tank steel was investigated in a series of environments designed to simulate the chemistry of legacy nuclear weapons production waste. Tests consisted of both slow strain rate tests using tensile specimens and constant load tests using compact tension specimens. Based on the tests conducted, nitrite was found to be a strong SCC inhibitor. Based on the test performed and the tank waste chemistry changes that are predicted to occur over time, the risk for SCC appears to be decreasing since the concentration of nitrate will decrease and nitrite will increase.

Keywords: stress corrosion cracking, carbon steel, nitrate, nitrite, pH, Hanford, nuclear waste

INTRODUCTION

The Hanford tank reservation contains approximately 50 million gallons of liquid legacy radioactive waste from cold war weapons production, which is stored in 177 underground storage tanks. Current plans call for eventual vitrification processing and ultimate disposal of the resulting waste glass logs at the Yucca Mountain Repository. The double shelled carbon steel storage tanks presently used for storage will continue in operation until the vitrification plant construction is finalized and waste processing operations completed.

Though there are several different waste chemistry types that have been grouped according to their main constituents, all of the wastes tend to be highly alkaline in nature, typically with pH values greater than 10 and to hydroxide concentrations in excess of 6M. Under alkaline conditions, carbon steels will tend to be passive and undergo relatively slow, uniform corrosion. Under these passive conditions, however, carbon steels also can become susceptible to localized corrosion (e.g., pitting) and stress corrosion cracking (SCC) in the presence of certain aggressive constituents, such as chloride and nitrate. The original single shell storage tanks experienced stress corrosion cracking failures as a result of the presence of high concentrations of nitrate in the waste. Research at Hanford and SRL demonstrated that cracking could be prevented by maintaining a high pH of the waste (>13) and post-weld heat treatment of the tanks.[1] Accordingly, all of the double shelled storage tanks were fabricated with stress relieved welds and chemistry controls were instituted to maintain the pH of the waste above 13-13.5 (as reflected as a minimum hydroxide concentration) in combination with a minimum nitrite concentration. At lower pH values, it was unclear if the relationships developed for higher alkaline conditions would still apply.

Due to various chemical reactions taking place inside the tanks, the waste chemistry will tend to change over time, especially given the currently estimated 2023 time horizon anticipated for tank operations to continue. In addition, the present chemistries for some of the tank waste types are no longer in specification with respect to corrosion (e.g., maintaining pH levels above 13-13.5). Thus, there is concern within DOE and regulatory bodies that tank integrity will be compromised given these changes in chemistry. Furthermore, if tank integrity is potentially compromised, there is a need to define mitigation procedures. Thus, the objective of this work was to determine the range of conditions where the tank steel is susceptible to localized corrosion and SCC to define possible corrosion mitigation strategies in the supernatant and sludge regions. The main focus of this paper is with respect to the risk for stress corrosion cracking with the results related to localized corrosion presented elsewhere.[2,3]

EXPERIMENTAL APPROACH

Materials and Solution Composition

A combination of slow strain rate tests (SSRT) using traditional tensile-type specimens and constant load crack growth rate tests (CGR) using compact tension specimens was performed. All test specimens were fabricated from three 3'×2'×1" as-supplied plates of ASTM A537 Class 2 carbon steel material that had been heat-treated to obtain material properties similar to those of the Class 1 carbon steel used for construction of the double shell storage tanks. The SSRT specimens were fabricated such that the longitudinal axis was in the plate rolling direction (i.e., longitudinal orientation). Compact tension specimens were fabricated such that the machined and fatigue precrack was in the plate rolling direction (i.e., transverse-longitudinal orientation).

Four main solution chemistries were simulated examined based on the present and the predicted future endpoint (assumed to be 2023 when vitrification operations are scheduled to begin) chemistry of two tank wastes. The future endpoint chemistries were determined using thermodynamic speciation calculations.[4] The main difference between the tank wastes is the chloride concentration whereas the endpoint wastes had a slightly depressed pH level, a decreased nitrate concentration, and an increased nitrite concentration. The main variables and the levels investigated are shown in Table 1. It should be noted that the simulated solutions contained 37 different chemical compounds and were allowed to mix on a shaker table for 24 hours prior to use. Additional details concerning the solution chemistries and their makeup can be found elsewhere.[3] All tests were conducted at 50 °C under quiescent conditions.

Slow Strain Rate Testing

SSR testing was performed according to the guidelines provided in ASTM G129[5] using cylindrical tensile specimens at a constant extension rate of 10^{-6} in/in-s. To perform the tests, a specimen was placed into a Teflon test cell and the load applied using pull rods that entered the cell through sliding seals. After insertion of the specimen and pull rods into the load frame, the solution of interest was introduced and heated to 50 °C. Tests were either conducted at open circuit or at an applied potential using SCE maintained at room temperature using a Luggin probe/salt bridge that was filled with the test environment solution. A platinum flag was used as a counter electrode.

Post-test analysis consisted of stereographic optical examination at 20 – 40x. Additional analyses using higher magnification optical microscopy, metallographic cross sectional analysis, and scanning electron microscopy (SEM) were also used on an as-needed basis. In cases where evidence of SCC was present, metallographic cross sectional analysis was utilized to estimate a crack growth rate by dividing the maximum crack length observed by the time to failure (total test time). Note that the crack growth rates determined from the SSR tests should be used with caution and only for comparative purposes. Furthermore, the crack growth rates estimated from the SSR test results should not be compared with the rates determined in the constant load crack growth rate tests using compact tension specimens. The SSRT CGRs tend to be higher because of the imposed continued straining of the specimens; a condition unrealistic for storage tanks. On the other hand, the cracks were assumed to initiate at the beginning of the test and continue to propagate at a constant rate throughout which will tend to underestimate the cracking rate in the SSR tests. This underestimation will tend to be exacerbated by the uncertainties associated with low probability of finding the longest crack in the specimen using metallographic cross-sectioning.

The time-to-failure and the strain at failure of the specimens did not always reflect clearly if SCC was present. Also, the degree of SCC was not easily established from these parameters. Therefore, the occurrence of SCC was always confirmed by visual inspection, and the severity of SCC was determined from the estimated crack growth rate. It was found from inspection of metallographic cross-sections of specimens that all cases where SCC was observed, intergranular features were also associated with the cracks.

Constant Load Crack Growth Rate Testing

Crack growth rate tests were performed using pre-cracked ½-T (0.5-inch wide) compact tension (CT) specimens subjected to a constant tensile load. In the CGR tests, crack extension as a function of time was measured using the DC potential drop (DCPD) technique. In this technique, a high electrical current (20 A) is sent through the specimen and the electrical potential between the two sides of the

crack is recorded. As a crack propagates the cross sectional area will decrease thereby increasing the resistance which is then measured as an increase in the potential drop across the specimen. Because the current passes through the specimen only, and not through the solution, this current does not affect the polarized potential of the specimen. The resistance increase causes an increase in the DCPD which can be related to the crack extension using the Johnson Equation.[6]

All tests were conducted in Teflon cells to which the environment was added and heated to the test temperature of 50 °C prior to applying the desired load. Tests were conducted either at open circuit or at an applied potential. For the tests at the open circuit potential, the potential was monitored with a high impedance voltmeter and a reference electrode (SCE). The electrode was maintained at room temperature and communicated with the test cell by means of a Luggin probe/salt bridge that was filled with the test environment. For the tests at applied potential, an additional platinum flag counter electrode was included in the cell and a potentiostat was used to control the potential to the desired value. All CGR experiments were performed under quiescent (no gas purging) conditions.

Post-test analysis was performed by initially sectioning the specimens longitudinally using a slow speed diamond saw. That is, the specimens were sectioned approximately at the center line of the thickness dimension creating two specimen halves. The face of one specimen half was then metallographically prepared to evaluate the microstructure of the steel and the SCC crack morphology (i.e., intergranular or transgranular). The other specimen half was mechanically overloaded in air to failure to expose the fracture surface for subsequent examination and analysis.

RESULTS AND DISCUSSION

The effects of different environmental variables and applied potential on the propensity and crack growth rate of SCC of tank steel in simulated high level nuclear waste from cold war weapons production is presented. The effect of potential (both applied and at open circuit) was examined as a possible key variable since classical SCC theory links susceptibility to the potential ranges near the active/passive transition and near the breakdown (or pitting) potential. The pH was evaluated since the tank chemistry specifications call for highly alkaline conditions to prevent SCC and the pH at present is out of specification and is predicted to continue to drift to lower values without active intervention. It was speculated that the pH shift away from the specification did not pose a significant immediate SCC threat due to the relatively high total organic carbon (TOC) concentration in the tanks which were theorized to provide some inhibition. The nitrate and nitrite were evaluated because their concentrations (an the concentration ratio) will change with time and nitrate is a known to promote SCC of carbon steel under alkaline conditions.[7,8,9,10]

Effect of Applied Potential on SCC

The applied potential was found to significantly influence the susceptibility of A537 to SCC. The estimated crack growth rate in the present day AN-107 tank simulated waste at pH 11 as a function of applied potential is shown in FIGURE 1. For comparison purposes, the corrosion potentials typically measured in AN-107 simulant solutions was between -150 and -225 mV vs. SCE. It should be noted that these corrosion potentials are higher than those measured in the tank which typically are on the order of -300 mV.[11] At potentials at or more negative than -100 mV vs. SCE, no SCC was observed (FIGURE 2) in any test in the AN-107 simulant solutions even at applied Ks as high as 40 ksi$\sqrt{in}$ (see FIGURE 3). The only instances where SCC was observed at potentials more negative than -100 mV have been in solutions with no or very low nitrite concentrations. For example, at open circuit (drifting from -500 to -

300 mV vs. SCE) in 5M $NaNO_3$ the crack growth rate was measured to be on the order of 5 x 10^{-8} in/s in a 30 day constant load test using compact tension specimens at an applied K of 40 ksi$\sqrt{in}$. The post-test appearance of the specimen from this test is shown in FIGURE 4. From FIGURE 1 it is also evident that the estimated CGR tends to increase with increasing (more noble) applied potential once the apparent cracking threshold potential of -100 mV is exceeded. Similar results have been reported by James and Moshier with respect to corrosion fatigue crack growth.[12] Based on linear regression of the data, the estimated crack growth rate will generally increase by about 4.4 x 10^{-7} mm/s for every 100 mV increase in potential (r^2 = 0.899). Though it appears that the crack growth rate increases with increasing potential, it must be cautioned that this trend might not continue at higher potentials. Furthermore, the engineering relevance of these higher potentials from a tank integrity perspective is diminished when the typical potentials measured in the tank are considerably lower.

The observation that SCC occurs above a critical potential and is absent below this potential is consistent with the reported observations of Cragnolino et al.[13,14] and Nakayama et al.[15] In these works, a clear link between the repassivation potential for localized corrosion and the critical potential for SCC was established for stainless steels and Ni-Cr alloys in chloride environments. Though some similarities between the present work and these exist (e.g., carbon steel is passive in alkaline environments and stainless steels and Ni-Cr alloys are also passive, chloride is present in both cases), this relationship between pitting and SCC from a repassivation potential does not seem to hold under all conditions for the present work. For example, in AN-107 simulant at pH 11 the repassivation potential and the critical potential for cracking are within 50 mV of each other (E_{rp}=~+50 mV vs. E_{SCC}=~0 mV). However, in other cases (e.g., AN-107 endpoint solution) the difference between E_{rp} and E_{SCC} was quite large (+215 vs. 0 mV respectively). Thus, even though there is a clear threshold potential for SCC, it may not be intimately tied to repassivation. It is interesting to note, however, that Nakayama et al.[15] noted a consistent potential offset between E_{rp} and E_{SCC} on the order of 100 mV with E_{SCC} always lower.

Effect of Solution pH

The effect of pH on the estimated crack growth rate from SSR tests in the standard AN-107 solution is shown in FIGURE 5. If the effect of applied potential is neglected and the data examined as an aggregate set, pH can be seen to have an inhibitive effect on SCC over the range of 7 to 11. For example, at an applied potential of +100 mV increasing the pH from 7 to 11 resulted in a decrease in the average estimated CGR from 5 x 10^{-6} to 8.5 x 10^{-7} mm/s. Additional increases in pH beyond 11 to values as high as 13.5, however, had no appreciable effect. Thus, the estimated CGR at an applied potential of 0 mV at pH 10 and 13.5 were nearly identical at 1 x 10^{-6} and 9 x 10^{-7} mm/s. The observations from SSRT testing were confirmed using compact tension specimens at applied Ks of 20, 30, and 40 ksi$\sqrt{in}$ where no significant differences in crack growth rate were noted when comparing pH 10 and 11. Similar results were shown by Ondrejcin[10] who noted that the ultimate tensile strength of steel held galvanostatically at 0.2 mA/cm^2 in nitrate solutions at 100 °C increased with increasing hydroxide concentration up to approximately 1.5M after which further increases did not provide any additional benefit. Thus, one possible explanation why no significant SCC has been observed in tanks containing this waste chemistry at Hanford though the pH level is below the specification might be because over the range that the pH has changed (13.5 vs. 11) there is little influence on SCC susceptibility especially when coupled with the low corrosion potential measurements that have been observed in the tank waste.

Effect of Total Organic Carbon

Because high organic carbon[a] levels were thought to inhibit SCC sufficiently to allow the AN-107 tank chemistry to fall out of pH specification, the effects of TOC levels on SCC were investigated. Though some possible improvements in SCC resistance were noted in the stress-strain behavior with increased TOC levels in some cases, there appears to be little influence of TOC levels on SCC rates with estimated CGRs ranging between $4 - 7 \times 10^{-7}$ mm/s for TOC levels of 10 – 80 g/L. Thus, it was concluded that high TOC levels were not a significant inhibitor for SCC.

Effect of Nitrite and Nitrite/Nitrate Ratio

Nitrite concentration and the nitrite/nitrate concentration ratio were found to have a pronounced influence on SCC susceptibility. FIGURE 6 shows the effects of the nitrite/nitrate concentration ratio as a function of applied potential on SCC susceptibility. These data show that at very low nitrite/nitrate ratios, the potential where SCC is observed extends to lower values. Conversely, as this ratio increases the SCC threshold potential increases. Thus, at any given potential, SCC can be mitigated by increasing the nitrite/nitrate ratio and at a constant nitrite/nitrate ratio the propensity for SCC decreases with decreasing potential. As the nitrite/nitrate ratio increases the difference between open circuit and the cracking potential widens thereby decreasing the risk for SCC. This is particularly the case since the open circuit potential has been observed to be essentially independent of the nitrite/nitrate ratio.[2]

When examined strictly from a nitrite concentration perspective, the inhibition provided by increased nitrite concentrations becomes evident (FIGURE 7 and FIGURE 8). At low nitrite concentrations, severe SCC is observed based on the stress-strain behavior (as shown in FIGURE 7) along with significant degradation of the sample. The beneficial effects of nitrite are immediately apparent even at concentrations as low as 0.35M (which equates to a nitrite/nitrate concentration ratio of approximately 0.095) when examining the stress-strain behavior though, it is unclear what influence nitrite has on CGR at these levels. Additional increases in the nitrite concentration to 0.875M and higher resulted in the stress-strain behavior becoming similar to that observed in air along with decreases in the estimated CGR. For example, at an applied K of 40 ksi$\sqrt{in}$, the crack growth rate was observed to decrease by a factor of 100 by increasing the nitrite/nitrate ratio from zero to 0.32. Concomitant with the observed decreases in the overall crack growth rate, the extent of cracking also decreased as shown in FIGURE 9and FIGURE 10. The intergranular nature of the cracking is also clearly evident in FIGURE 9. In contrast to the more aggressive conditions where multiple secondary cracks were often observed in SSR tests with low nitrite, often times only a single secondary crack (if any) were noted at higher nitrite concentrations. Eventually, complete inhibition of SCC was achieved at nitrite concentrations that approached the nitrate concentration (near a nitrite/nitrate ratio of 1).

The noted inhibition from nitrite was recognized by Ondrejcin[10], but the magnitude of this inhibition was not noted in his work nor was any speculation regarding the possible inhibition mechanism discussed. Though efforts to elucidate the mechanism by which nitrite provide SCC inhibition, both of the following reactions are possible under the conditions investigated:

$$2NO_2^- + 3H_2O + 4e^- \rightarrow N_2O + 6OH^-$$

$$NO_2^- + 5H_2O + 6e^- \rightarrow NH_3 + 7OH^-$$

[a] In the simulated waste, the organic carbon was added as EDTA (ethylenediaminetetraacetate), HEDTA (n-hydroxyethylenediamine triacetate), sodium gluconate, glycolic acid, citric acid, nitrilotriacetic acid, iminodiacetic acid, sodium formate, sodium acetate, and sodium oxalate.

Each of these reactions result in the production of hydroxide thereby possibly providing added buffering capacity at the crack tip and promoting passivity or repassivation. Additional work is planned to evaluate this further.

Effect of Chloride

The effect of chloride on SCC was examined over the range of 0.05M (present concentration in the AN-107 tank) to 0.2M (present concentration in the AN-102 tank). Cracking propensity in both standard and endpoint solutions was studied. In addition, one test was run with higher chloride and an applied potential of -100mV to evaluate which of the two parameters had a greater effect on SCC susceptibility.

Changing the chloride concentration over the range of 0.05 to 0.2M did not have an appreciable effect on SCC behavior, as measured through changes in the estimated crack growth rate (FIGURE 11). Reducing the chloride concentration from 0.1M to 0.05M did not have a significant effect on the estimated crack growth rate. Increasing the chloride concentration from 0.1M to 0.2M had mixed results with one specimen exhibiting major SCC (the specimen was severely corroded after testing and an estimated crack growth rate could not be determined from cross sectional analysis and a value of 10^{-5} mm/s was assumed). In a duplicate test at 0.2M chloride and 0 mV vs. SCE, moderate SCC was observed with an estimated crack growth rate comparable to the other chloride concentrations evaluated. However, the SCC in the higher chloride solution appeared to be eliminated by reducing the applied potential to -100mV vs. SCE. This observation is consistent with other tests conducted at -100 mV. The effect of chloride concentration on constant load crack growth rate testing using compact tension specimens was also found to be insignificant. Given the small range in chloride concentration investigated and that SCC appears to be controlled primarily by the nitrate/nitrite ratio it is not surprising that little effect of chloride was observed in the present work.

Effect of Stress Intensity

The effect of applied K was explored in an attempt to define the critical threshold intensity factor for SCC (K_{ISCC}). Based on the results obtained (FIGURE 12), no crack growth was detected at 5 ksi$\sqrt{in}$. At higher applied Ks, the crack growth became detectable at 10 ksi$\sqrt{in}$ but still at slow rates. Additional increases in K above 10 ksi$\sqrt{in}$ did result in an increase in the crack growth rate but essentially there were no additional rate increases with higher K values above 20 ksi$\sqrt{in}$. It is unclear from these data precisely what the value of K_{ISCC} is in either standard or endpoint solutions but it appears to be between 10 – 20 ksi$\sqrt{in}$, though it could also lie between 20 – 30 ksi$\sqrt{in}$. Despite the uncertainties in the determination of K_{ISCC} in the present work, good agreement with the values reported by Donovan who estimated K_{ISCC} in similar environments to be between 33 – 42 ksi$\sqrt{in}$ using optical inspection of wedge open load specimens.[16]

These estimates of K_{ISCC} can be used in conjunction with stress analyses and fracture mechanics to calculate the critical flaw size necessary for SCC.[17] Utilizing the approach adopted by Rinker et al.[16] if K_{ISCC} is assumed to be between 20 and 30 ksi$\sqrt{in}$, and a residual stress of 10 ksi and a 0.5 inch wall thickness in the lower knuckle region of the tank were also assumed, a crack would have to be between 0.15 and 0.25 inches (respectively) for SCC to occur. The upper limit on crack growth rate measured in the recent tests is approximately 2×10^{-9} in/s. If a crack of the critical size were present it would propagate and result in through wall penetration in approximately 4 to 5.5 years.

It is possible that crack tip blunting effects will influence the measured crack growth rates. Intuitively, it would be expected that a higher applied K would provide a greater driving force for crack propagation. However, a high stress near the crack tip can lead to blunting of the crack tip and a reduction in the effective localized applied K. This may explain why the crack growth rates for applied Ks between 20 and 40 ksi$\sqrt{in}$ are essentially the same.

SUMMARY AND CONCLUSIONS

Based on the work conducted, the key findings are:

- No SCC was observed under open circuit conditions in any of the AN-107 simulants; additionally, the corrosion potentials measured in actual tank waste tended to be at least 60 mV more negative than those measured in the waste simulants under similar conditions (quiescent, non-deaerated conditions)

- Nitrite has been found to be a strong inhibitor for SCC
  - Nitrite/nitrate concentration ratios near 1.0 were found to impart substantial resistance
  - Though nitrite/nitrate ratios around 1.0 were found to be beneficial, it is uncertain based on the data obtained thus far if the concentration ratio or the absolute concentration of nitrite controls inhibition

- pH appears to act as an inhibitor for SCC
  - Increasing the pH over the range from 7 – 11 in standard AN-107 solutions resulted in a decrease in the estimated crack growth rate in SSR tests; above pH 11 there did not appear to be an influence of pH on the SCC crack growth rate
    - In the simulated endpoint AN-107 chemistry, pH values as low as 9.5 showed estimated crack growth rates comparable to those observed in standard AN-107 simulant at pH 11 (this appears to be due to the greater nitrite/nitrate ratio in the endpoint chemistry compared to the standard simulant chemistry)

- TOC appears to provide some inhibition of SCC under some circumstances but otherwise has a negligible influence

- Applied potential is an important factor in establishing regions of SCC susceptibility
  - At potentials more negative than -100 mV vs. SCE, SCC was not observed in AN-107 solutions
  - More positive applied potentials (than -100 mV) not only induces SCC but the estimated crack growth rate increased with increasing potential
  - No SCC was observed in any of the AN 107 solutions at the free corrosion potential

- Chloride concentration was shown to have a minimal effect on SCC over the range of 0.05 to 0.2M in AN-107/AN-102 simulants

- SCC was observed in simulated AN-107 standard and endpoint solutions with a maximum crack growth rate of ~ 2×10^{-9} in/s in constant load tests
  - The crack growth rate in the constant load tests was relatively independent of applied K above 20 ksi$\sqrt{in}$

- Based on the testing conducted, K_{ISCC} is estimated to be between 10 and 30 ksi$\sqrt{in}$ (most likely near 20 ksi$\sqrt{in}$)

Based on the results obtained, it appears that as the chemistry continues to change with time the risk for SCC will be decreasing since the nitrite/nitrate ratio will be steadily increasing. This should counter the slight negative effects of the pH continuing to decrease from around a present value of 11 to a predicted future value of 10. This assertion is further bolstered by the observation that the simulated endpoint chemistries were at pH 10 and the critical potential for the occurrence of SCC was noted to increase from -100 mV to -50 mV vs. SCE.

TABLE 1: SUMMARY OF MAIN CONSTITUENTS IN THE WASTE SIMULANTS INVESTIGATED IN THE PRESENT WORK

Solution	Baseline Solution Chemistries				
	Nitrate (M)	Nitrite (M)	Chloride (M)	Total Organic Carbon (g/L)	pH
AN-107 Present	3.7	1.2	0.1	20	11
AN-107 Endpoint	2.4	2.3	0.1	20	10
AN-102 Present	3.7	1.2	0.2	20	11
AN-102 Endpoint	2.4	2.3	0.2	20	10

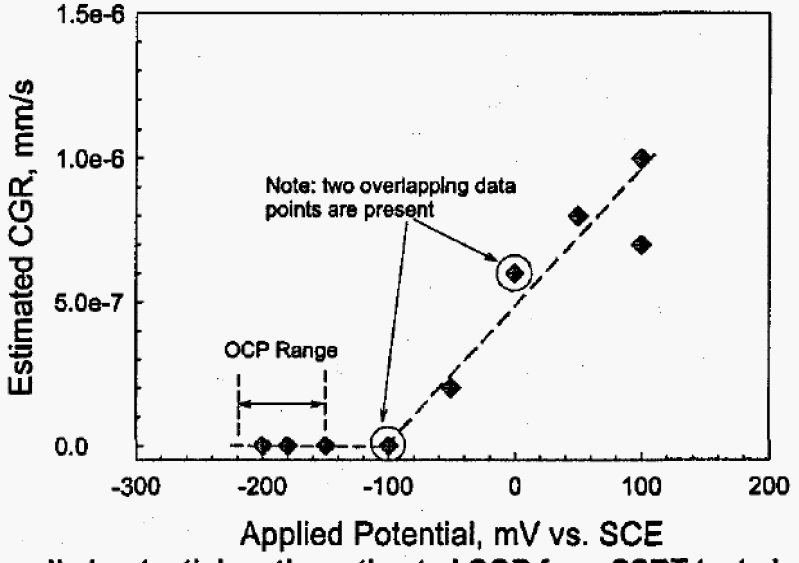

Figure 1: Effect of applied potential on the estimated CGR from SSRT tests in AN-107 at pH 11.

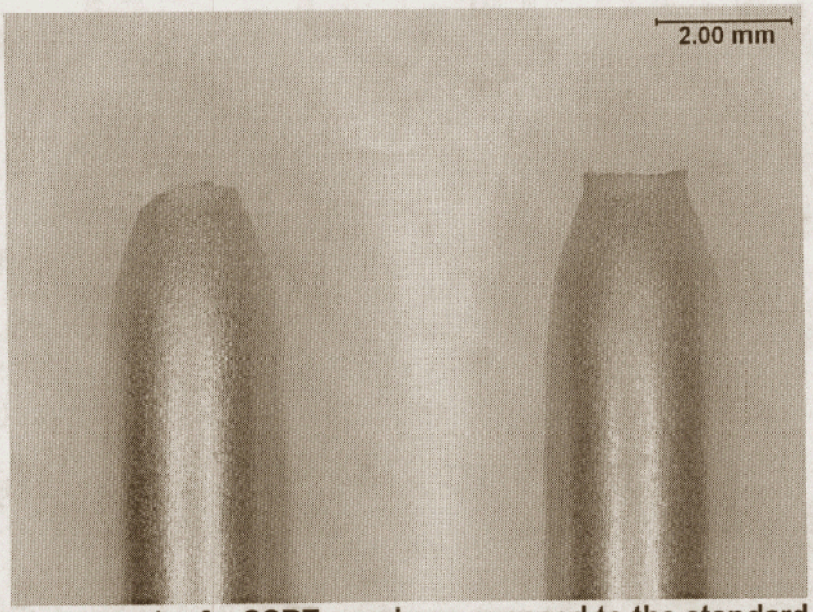

Figure 2: Post-test photograph of a SSRT specimen exposed to the standard AN-107 solution at open circuit and 50 °C.

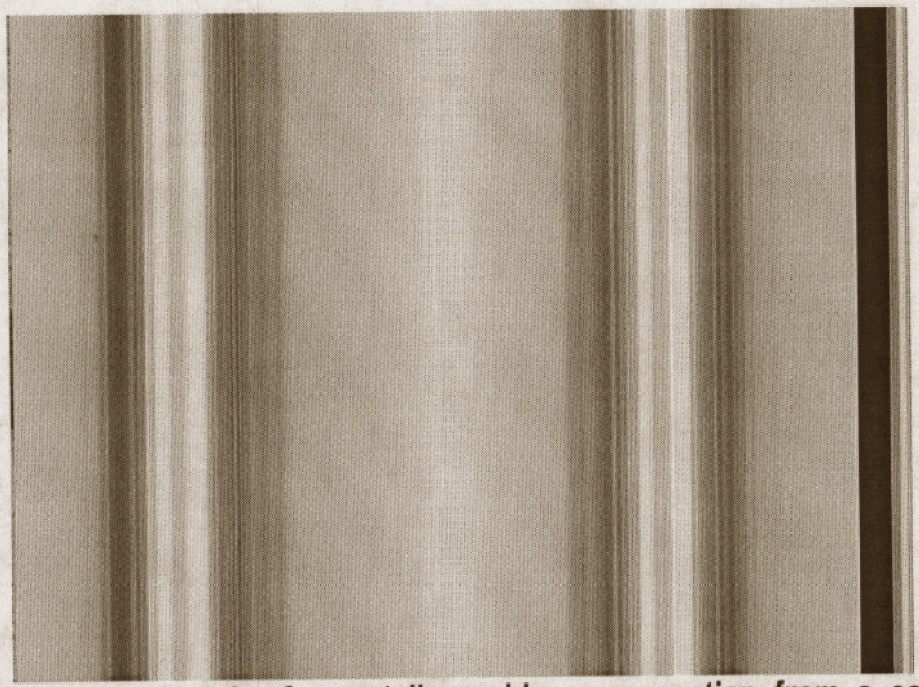

Figure 3: Post-test micrograph of a metallographic cross section from a compact tension specimen exposed to the simulated endpoint AN-107 solution at open circuit at an applied K of 40 ksi$\sqrt{in}$. No SCC is observable (the crack that is present is the original fatigue pre-crack emanating from the EDM notch on the left).

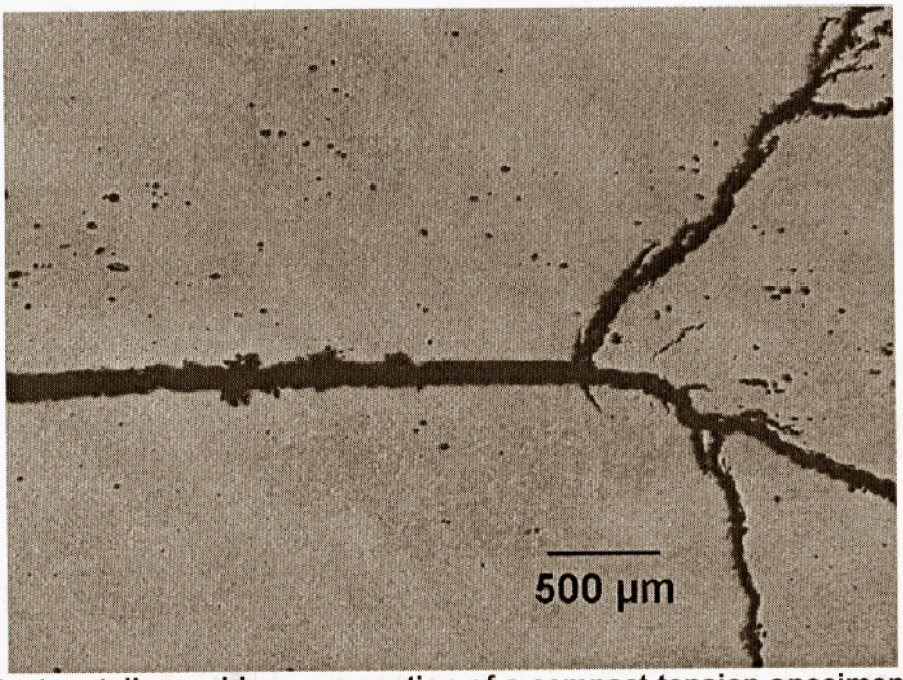

Figure 4: Post-test metallographic cross section of a compact tension specimen exposed to 5M $NaNO_3$ at open circuit at an applied K of 40 ksi√in showing evidence of significant SCC and crack branching.

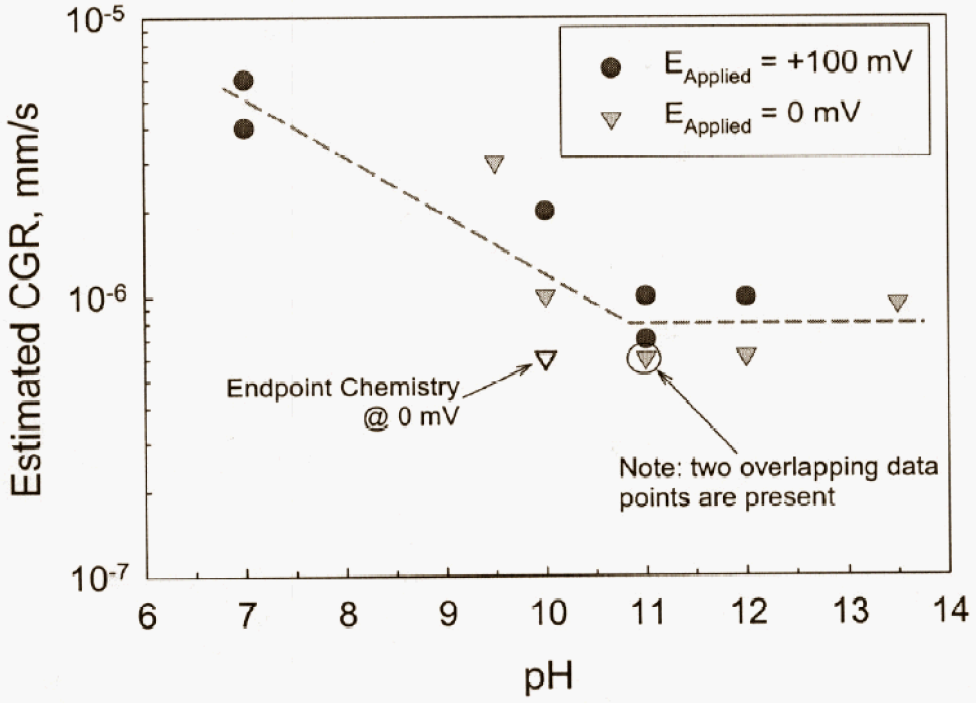

Figure 5: Effect of pH on the estimated CGR in AN-107 standard solution. Also shown is the estimated crack growth rate determined in the -AN-107 endpoint simulant at pH 10 and an applied potential of 0 mV.

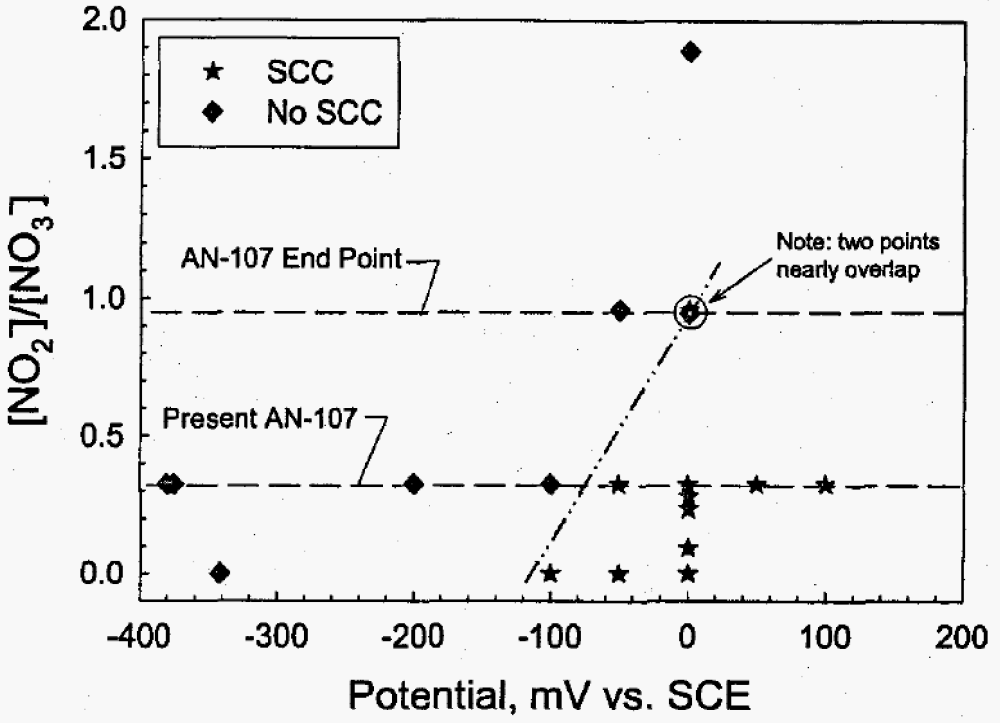

Figure 6: Effect of nitrite/nitrate concentration ratio on the propensity for SCC in Tank 241-AN-107 solution as a function of applied potential (both standard Tank 241-AN-107 and endpoint Tank 241-AN-107 are included).

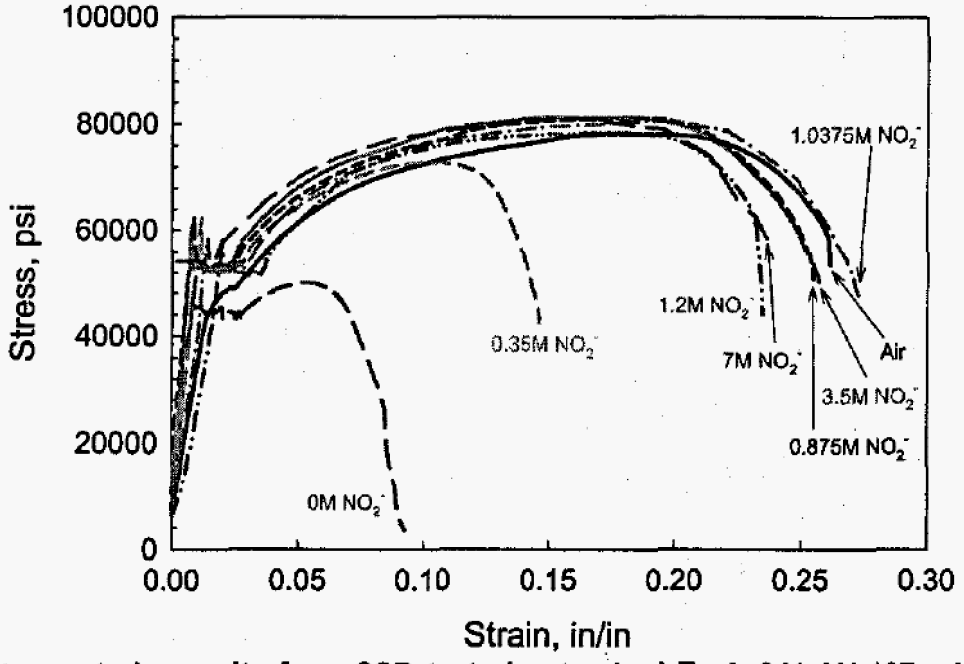

Figure 7: Stress-strain results from SSR tests in standard Tank 241-AN-107, pH 11 solutions with different nitrite concentrations at 0 mV.

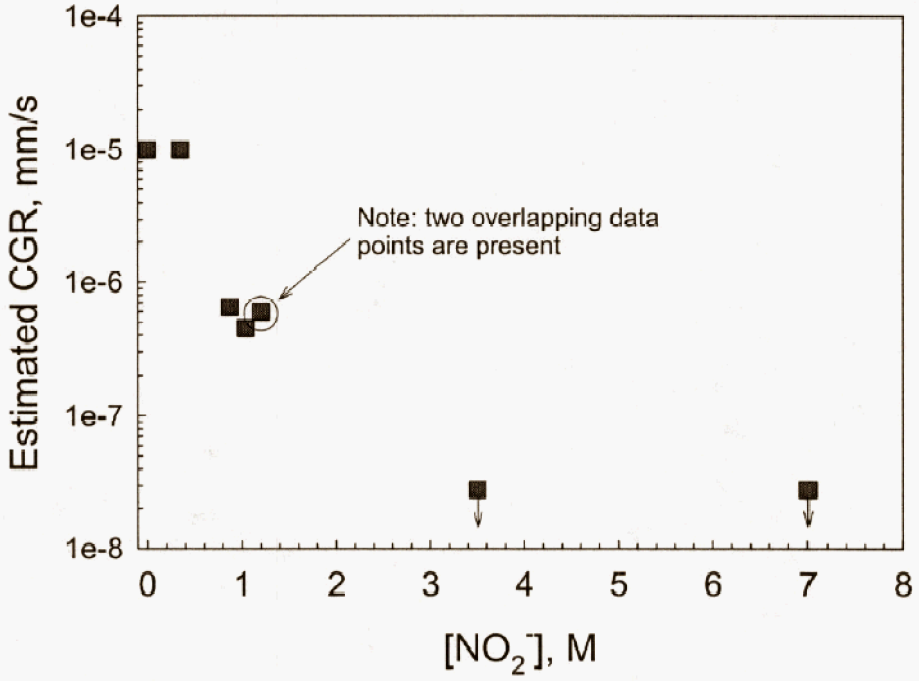

Figure 8: Effect of nitrite concentration on estimated CGR from SSR tests in standard Tank 241-AN-107 at pH 11 and an applied potential of 0 mV. Note that the CGR could not be estimated for the tests at 0 and 0.35M nitrite due to excessive degradation of the specimens and thus a value of 10^{-5} mm/s was assumed. Furthermore, no SCC was found at nitrite concentrations of 3.5 and 7M as denoted by the downward arrows.

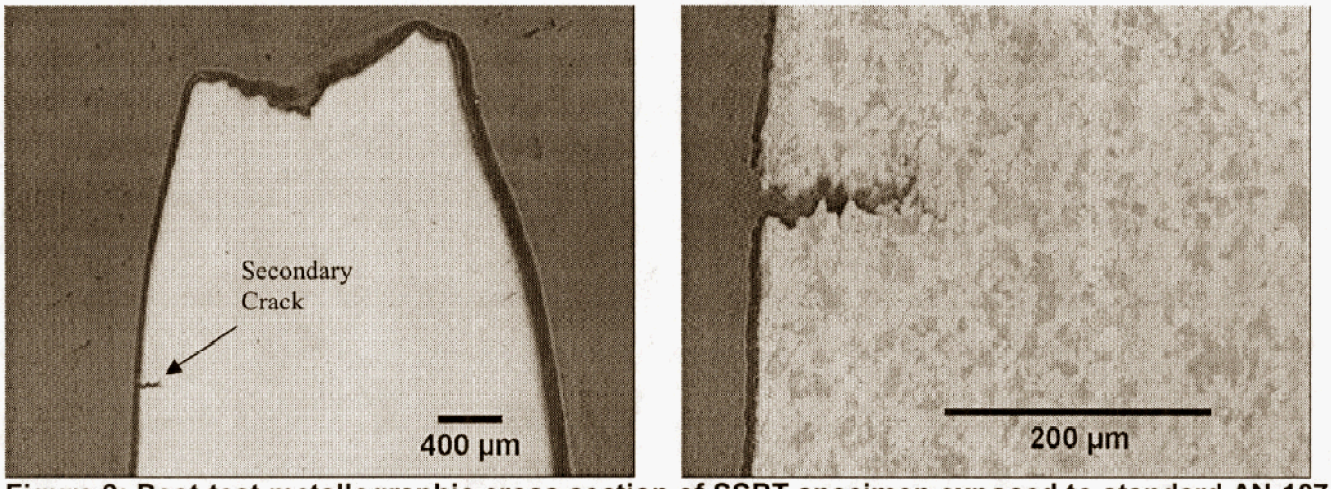

Figure 9: Post-test metallographic cross section of SSRT specimen exposed to standard AN-107 simulant at pH 11 and an applied potential of 0 mV vs. SCE.

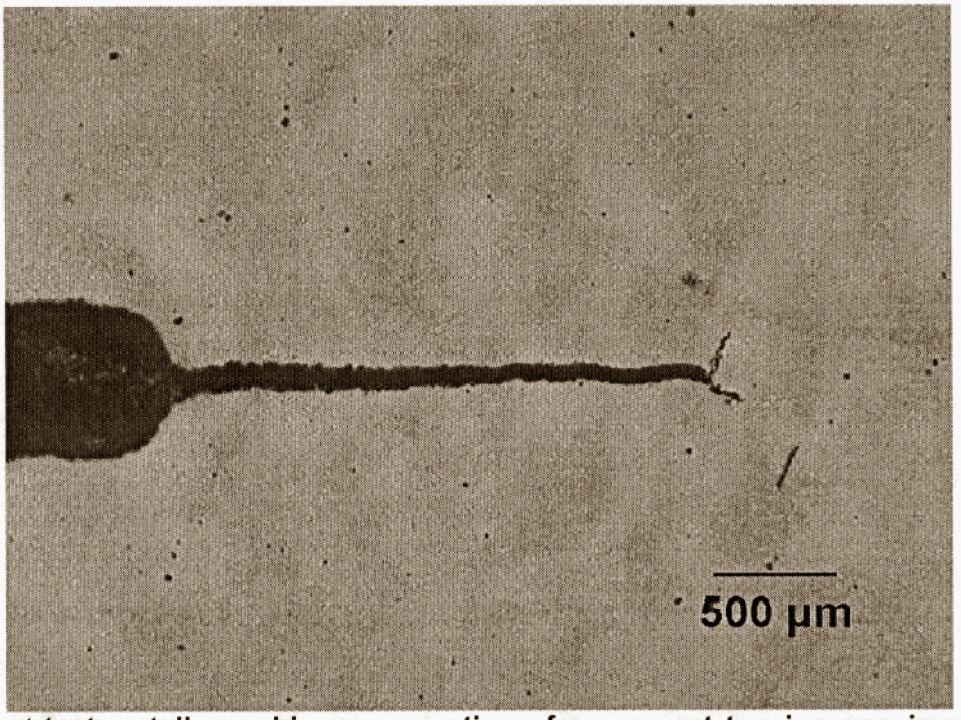

Figure 10: Post-test metallographic cross section of a compact tension specimen exposed to AN-107 standard simulant at pH 10 and an applied potential of 0 mV at an applied K of 40 ksi√in for 30 days.

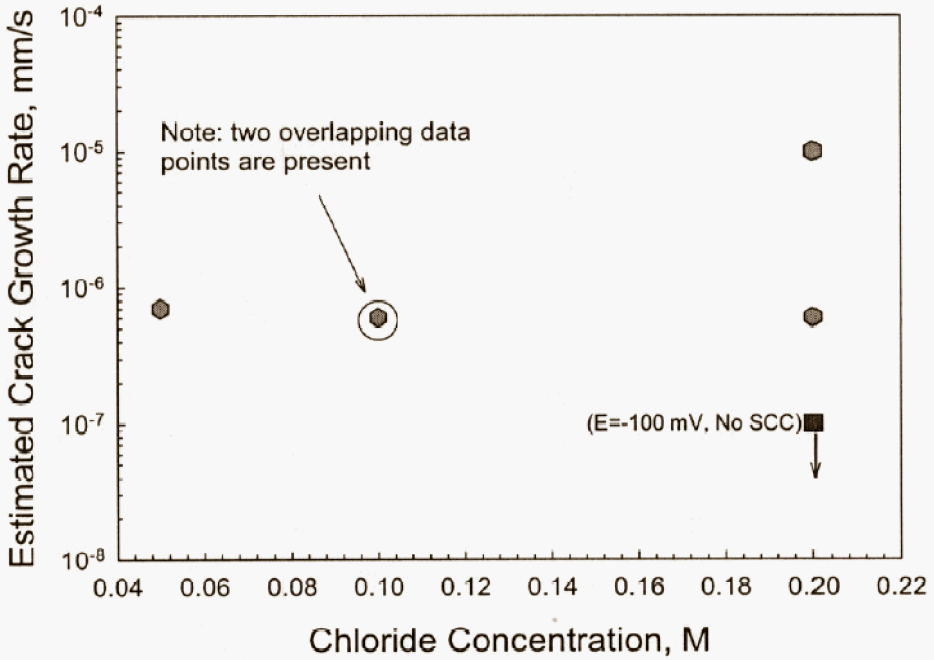

Figure 11: Effect of chloride concentration on the estimated crack growth rate in pH 11 Tank 241-AN-107 solutions at 50 °C. All tests (except one) were performed at an applied potential of 0 mV vs. SCE.

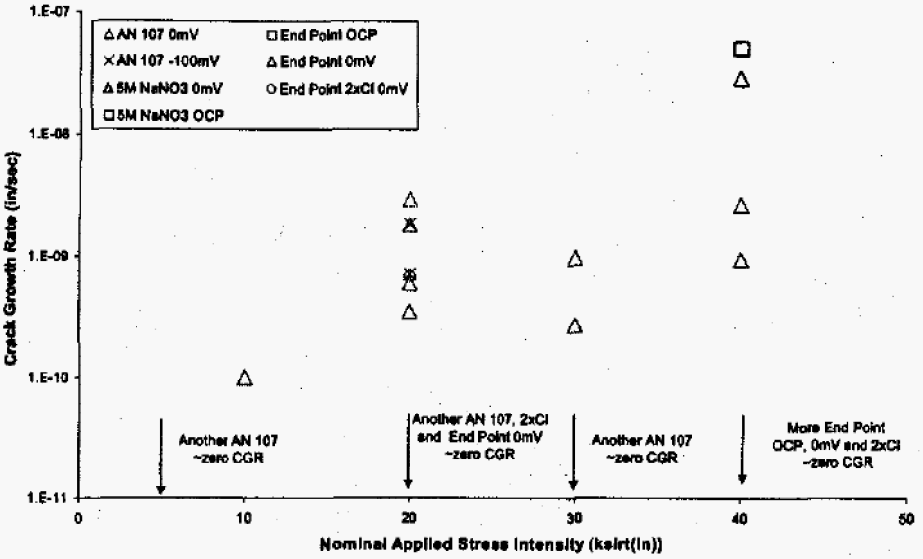

Figure 12: Effect of applied K on the crack growth rate determined using DCPD (using DCPD data after the initial 5 days of testing).

REFERENCES

[1] R.E. Eibling and C.A. Nash, Hanford Waste Simulants Created to Support the Research and Development on the River Protection Project – Waste Treatment Plant, WSRC-TR-2000-00338, Westinghouse Savannah River Company, Aiken, SC (2000).

[2] F. Gui, C.S. Brossia, J.A. Beavers, C. Mendez, G. Frankel, G. Edgemon, and H. Berman, "On the Anodic Polarization Behavior of Carbon Steel in Hanford Nuclear Wastes", Paper no. 07593, NACE Corrosion2007 (2007).

[3] C.S. Brossia, F. Gui, and C. Scott, Hanford Tanks 241-AN-107 and 241-AN-102: Effect of Chemistry and Other Variables on Corrosion and Stress Corrosion Cracking, Report 805062, CC Technologies, Dublin, OH (2006).

[4] Letter from Leon

[5] Standard Practice for Slow Strain Rate Testing to Evaluate the Susceptibility of Metallic Materials to Environmentally Assisted Cracking, ASTM International (2005).

[6] H.H. Johnson, *Materials Research and Standards*, vol. 5, No 9, September 1965, pp. 442-445.

[7] J.J. Kropowicz, R.M. Davis, and D.N. Hopkins, *Scripta Metallurgica et Materialia*, vol. 25, p. 1501 (1991)

[8] R.N. Parkins, in Stress Corrosion Cracking and Hydrogen Embrittlement of Iron Base Alloys, NACE-5, p. 601, NACE International, Houston, TX (1977).

[9] M.L. Holzworth, R.M. Girdler, L.P. Costas, and W.C. Rion, *Materials Protection*, January, p. 36 (1968).

[10] R.S. Ondrejcin, in Stress Corrosion Cracking – The Slow Strain Rate Technique, ASTM STP 665, p. 203, ASTM International, West Conshohocken, PA (1979).

[11] J.B. Duncan, Electrochemical Corrosion Testing of A537 Class 1 Carbon Steel in 241-AN-107 Sludge, CH2M Hill Report FH-0300284 (2003).

[12] L.A. James and W.C. Moshier, *Corrosion Science*, vol. 41, p. 373 (1999).

[13] G. Cragnolino, D.S. Dunn, and N. Sridhar, Corrosion, vol. 52, p. 194 (1996).

[14] G.A. Cragnolino, D.S. Dunn, Y.-M. Pan, and N. Sridhar, in Chemistry and Electrochemistry of Corrosion and Stress Corrosion Cracking: A Symposium Honoring the Contributions of R.W. Staehle, p. 83, R.H. Jones (ed.), TMS Annual Meeting, New Orleans (2001).

[15] G. Nakayama, C. Liang, and M. Akashi, *Corrosion Engineering*, vol. 45, p. 345 (1996).

[16] J.A. Donovan, Resistance of Type A537 Class I Steel to Nitrate Stress Corrosion Cracking, E.I. Du Pont de Nemours and Company Report DPST-81-687-TL (1981).

[17] M. W. Rinker, J. E. Deibler, K. I. Johnson and S. P. Pilli, 2005. Evaluation and Recommendation of Stress Criteria for Stress Corrosion Cracking of Hanford Double Shell Tanks (draft report, Rev 0) Fig 5.4.